ACS APPLIED MATERIALS & INTERFACES

www.acsami.org

Research Article

Disruption of Electrospinning due to Water Condensation into the Taylor Cone

Catherine G. Reyes and Jan P. F. Lagerwall*

Cite This: *ACS Appl. Mater. Interfaces* 2020, 12, 26566–26576

Read Online

ACCESS | Metrics & More | Article Recommendations | Supporting Information

ABSTRACT: The well-known problems of electrospinning hygroscopic polymer fibers in humid air are usually attributed to water condensing onto the jet mid-flight: water enters the jet as an additional solvent, hindering solidification into well-defined fibers. Here, we show that fiber fusion and shape loss seen at the end of the process may actually stem from water already condensing into the Taylor cone from where the jet ejects, if the solvent is volatile and miscible with water, for example, ethanol. The addition of water can radically change the solvent character from good to poor, even if water on its own is an acceptable solvent. Moreover, and counterintuitively, the water condensation promotes solvent evaporation because of the release of heat through the phase transition as well as from the exothermic mixing process. The overall result is that the polymer solution develops a gel-like skin around the Taylor cone. The situation is significantly aggravated in the case of coaxial electrospinning to make functional composite fibers if the injected core fluid forms a complex phase diagram with miscibility gaps together with the polymer sheath solvent and the water condensing from the air. The resulting phase separation coagulates the polymer throughout the Taylor cone, as liquid droplets with different compositions nucleate and spread, setting up strong internal flows and concentration gradients. We demonstrate that these cases of uncontrolled polymer coagulation cause rapid Taylor cone deformation, multiple jet ejection, and the inability to spin coaxial fiber mats, illustrated by the example of coaxial electrospinning of an ethanolic polyvinylpyrrolidone solution with a thermotropic liquid crystal core, at varying humidities.

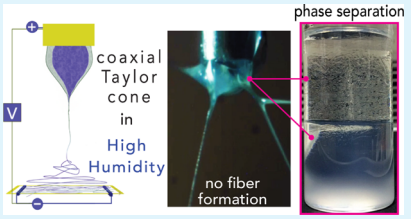

KEYWORDS: *Taylor cone, atmospheric humidity, coaxial electrospinning, multicomponent fluids, phase separation, water condensation, liquid crystals, hygroscopic polymer*

1. INTRODUCTION

Electrospinning and electrospraying methods continue to be popular for quickly producing composite fibrous membranes and particles with high specific surface area and with tuned multifunctionality enabled by coaxial modifications.[1−3] Here, a functional fluid, that is not readily spinnable on its own, is spun as a core inside a polymer solution, where the latter transforms into a solid cylindrical/spherical sheath during the spinning/spraying process, retaining and confining the core fluid in the final fiber/particle. The last two years have shown that these techniques are becoming more widely used, for example, in the fields of biotechnology and medicine to produce tissue scaffolds,[4] capsules for wound healing,[5] for diagnostic imaging,[6] and for conducting multicomponent drug release studies.[2,7,8] In the field of materials science, coaxial electrospinning is also a popular means of fabricating nonwovens that are responsive to external stimuli[9] such as temperature changes,[10−13] light,[14,15] gas exposure,[16−19] or sound waves[20] thanks to incorporated functional core liquids.

Considering the broad interest in, and large potential of, coaxial electrospinning/electrospraying, it is imperative to have a good understanding of the complex phenomena that may occur when the different precursor liquids are brought together during the process. However, such an understanding is still lacking, in particular, regarding the composite Taylor cone,[21,22] the electrostatically deformed droplet from which the jet making the fibers or particles is ejected. Here, the core and sheath liquids are in contact for several seconds prior to jetting. Both electrospinning and electrospraying are initiated from the Taylor cone, its formation being the initial response of the spinning/spraying fluid(s) to the electric field, imposed by applying an external potential (on the order of ∼10 kV) onto a metal capillary through which the spinning liquids flow, with a grounded collector plate placed at a distance of ∼10 cm away. When the surface tension of the liquid in the Taylor cone is overpowered by the electrostatic forces, a charged fluid jet shoots outward from the cone apex at a speed on the order of 10 m/s,[23] eventually discharging onto the collector plate as fibers or particles. In case of coaxial electrospinning or spraying, the core liquid must undergo the same distortion process inside the Taylor cone and get ejected from it together with the confining polymer sheath solution as the core of a composite jet. When this succeeds, fibers and particles with

Received: February 20, 2020
Accepted: May 18, 2020
Published: May 18, 2020

https://dx.doi.org/10.1021/acsami.0c03338
ACS Appl. Mater. Interfaces 2020, 12, 26566−26576

unique functionality can be produced. For instance, composite fibers with a liquid crystal (LC) core inside a polymer sheath produced by electrospinning comprise a versatile form factor enabling novel applications of these highly responsive liquids.[9,13,14,16,17,19,24−26]

Although scaling laws for tuning coaxial Taylor cones exist, based on the key electrospinning operating parameters and the chemical properties of the liquids,[27−29] these studies do not consider the possibility that the core and sheath liquids, or components thereof, mix, setting up concentration gradients and potentially leading to complex phase diagrams. Likewise, the full impact of water in humid air condensing onto the Taylor cone, coaxial or single-phase, as it cools down because of solvent evaporation is not taken into account. In fact, surprisingly many electrospinning activities are carried out with almost no attention to the Taylor cone and many reports give no information about its characteristics. The goal of this paper is to show that this approach misses a vital piece of information because instabilities in the Taylor cone, here triggered by humid air, can dramatically impact how the jetting progresses during spinning.

We first demonstrate that a single-phase Taylor cone formed by an ethanolic solution of polyvinylpyrrolidone (PVP) loses its shape stability and emits multiple jets if the ambient relative humidity (RH) surpasses values of about 70%, as a result of gel formation at the Taylor cone surface. We argue that the phenomenon arises because of heat release and deterioration of solvent quality as the water condenses from the humid air into the Taylor cone. We then move on to the case of coaxial electrospinning with an LC core, revealing that the presence of the core can render the spinning even more sensitive to water condensation, further reducing the maximum acceptable atmospheric humidity. We show that the liquid crystallinity per se is not the cause, instead attributing the effect to uncontrolled phase separation taking place when the core LC exhibits a broad miscibility gap in the phase diagram with ethanol and water. As many liquid combinations have such phase diagrams, in particular, the ternary phase diagrams arising when water is added to a nonaqueous solution, similar behavior can be expected with other functional core liquids. While we only examine the case of electrospinning of fibers, our results should apply equally to particle production by electrospray.

2. EXPERIMENTAL SECTION

2.1. Electrospinning Setup. All electrospinning experiments are carried out using a setup previously described in refs,[16,17] with schematics and photos shown in the Supporting Information. In brief, a stainless steel capillary with an outer diameter of 1.10 mm and inner diameter of 0.70 mm, and a polyimide-coated silica capillary with outer and inner diameters of 360 and 250 μm, respectively, are used to form the coaxial spinneret. The polymer sheath solution flows in the stainless steel capillary, whereas the LC core fluid flows in the silica capillary. While spinning the pure PVP fibers, the silica capillary is also physically present, but no core fluid is pumped through it. The steel capillary is electrically connected to a high-voltage power supply (Gamma High Voltage, Ormond Beach (FL), USA), and a sheet of aluminum foil (roughly 20 μm thick) is used as the grounded counter electrode (collector). Fibers are picked up for microscopic investigation on glass slides attached to the aluminum foil. The spinneret-to-collector distance is maintained at 12 cm, and the applied voltage is 9 kV for single-phase polymer fiber spinning and raised to 9.5 kV when the LC core is included. The spinneret is mounted horizontally in one wall of a Plexiglas box with dimensions 50 cm (height) by 45 cm (width) by 45 cm (length), and the whole box is placed within a fumehood. The ambient RH is tuned from 23 to 72% by inserting a humidifier (TaoTronics TT-AH002) inside the box such that it does not obstruct the path of the jet during spinning. The temperature is in the range of 21−23.8 °C. The temperature and humidity levels of the spinning area are monitored using a digital thermo-hygrometer (TFA Dostmann, model 30.5002).

The polymer solution and the LC fluids are kept in separate glass vials closed with septa-equipped caps. Each cap was punctured twice to allow for the delivery of air to the vial and to connect the tubes for flowing the LC fluid and polymer solution to the coaxial spinneret. A diagram of this coaxial setup with the solutions connected during use is shown in Figure S7 of the Supporting Information. Briefly, a hypodermic needle connected via a rubber tube to one channel of a pneumatic microfluidic control unit (MFCS-EZ, Fluigent, Paris, France) is inserted into the headspace of the polymer solution vial to pressurize it as desired. At the same time, another hypodermic needle connected via a polytetrafluoroethylene tube leading to the coaxial spinneret is inserted into the vial so that it is fully in contact with the polymer sheath solution. When the vial overpressurizes, the solution flows into the appropriate channel of the spinneret. The same process for flowing the LCs to the coaxial spinneret is also performed, with the only difference being that instead of a hypodermic needle being in contact with the LCs in the vials, the silica capillary, mentioned previously, flows the LCs directly from the vials to the spinneret. The polymer solution is flowed at a rate of 1.1 mL/h, for single-phase as well as coaxial spinning, and the LC flow rate is set at 0.55 mL/h. The combination of flow rates, voltage, and spinneret-to-collector distance was chosen to be well within a window of reliable spinning conditions, for the single-phase and coaxial cases, respectively, when the atmosphere is dry (RH < 50%).

2.2. Chemicals and Mixtures. PVP (weight average molar mass M_w = 1.3 × 10^6 g/mol, most commonly atactic[30]) is obtained from Sigma-Aldrich and dissolved in anhydrous ethanol (ethanol for molecular biology ≥99.8% purity, Merck, CAS #: 64-17-5) to create a 12.5% by mass solution. As reference, Asawahame et al. reported the surface tension of a 12% solution of the same quality of PVP in ethanol to be ∼26 mN/m,[31] Cengiz Çallioğlu and Kesici Güler reported 19 mN/m for 12% PVP with M_w = 0.36 × 10^6 g/mol in ethanol,[32] and Forward and Rutledge reported 23 mN/m for 8% PVP with M_w = 1.3 × 10^6 g/mol in ethanol[33] (none of the studies reported the measurement temperature). These figures can be compared to the surface tension of pure ethanol, 22.1 mN/m (http://www.surface-tension.de), suggesting a marginal effect of the PVP. The corresponding reported electrical conductivities and viscosities, respectively, were 11.9 μS/cm[a] and 1.2 Pa s,[31] 8.6 μS/cm and 0.46 Pa s[32] and 0.28 μS/cm[b] and 0.07 Pa s.[33]

The three LCs used were 4-cyano-4′-pentylbiphenyl (5CB), E7, and ROTN-403. All three LCs have a nematic phase at room temperature, but only 5CB is a single component, while E7 and ROTN-403 are mixtures (thus, they are only known by their commercial names). Significantly, E7 is partially comprised of 5CB, 47 mol % of the mixture being this molecule. While the other components are also molecularly similar, all containing cyano end groups, longer aliphatic chains or additional phenyl rings enable the nematic to isotropic transition temperature (clearing point, T_c) of the mixture to be much higher, expanding its nematic temperature range. The components of ROTN-403 are not fully known to us, as it is a proprietary commercial mixture, but it is miscible with 5CB and E7 at room temperature and its components are structurally similar.[34] 5CB and E7 were purchased from SYNTHON Chemicals GmbH, and confirmed to have, respectively, T_c^{5CB} = 35.6 °C and T_c^{E7} = 58 °C (start of the transition, which here is extended in temperature as E7 is a mixture). This was carried out using a Linkam T95 series LTS120E temperature control stage. The ROTN-403 mixture (T_c^{ROTN} = 81.5 °C; start of the transition) is no longer commercially available but was originally purchased from Hoffmann-La Roche.

The effective shear viscosities at room temperature of the three LCs range between 0.02 and 0.05 Pa s,[35] making them comparable to vegetable oils in terms of flow properties. Thus, they are all easy to flow at room temperature. The electrical conductivity of 5CB in the

https://dx.doi.org/10.1021/acsami.0c03338
ACS Appl. Mater. Interfaces 2020, 12, 26566−26576

isotropic phase was measured earlier by us to be 1.03 nS/cm,[9] thus 4 orders of magnitude lower than that of the PVP solution. The conductivities of the two LC mixtures are expected to be in the same range; hence, we can safely conclude that the PVP solution is the driving fluid, that is, the charges building up in the Taylor cone during electric field application segregate to the PVP solution−air interface, and it is the electrostatic Maxwell stress on the outer solution that drives the spinning, requiring it to be viscous enough to bring the LC core with it into the jet.[28]

All three LCs are completely insoluble in water. In anhydrous ethanol, 5CB is fully soluble and E7 partially soluble, whereas ROTN-403 has low solubility. We can thus expect very low interfacial tension between 5CB and E7 with the ethanolic sheath solution, while it may be somewhat higher for ROTN-403. Still, a very high interfacial tension is not expected, as the molecular structures are qualitatively similar in all LCs.[34] A detailed comparison of the LC miscibility in six solvents is shown in Figure S1 in the Supporting Information.

2.3. Taylor Cone Characterization. To monitor the Taylor cone in each experiment, a digital camera (Zarbeco, model: ZC-505-O2) was attached to a macro lens by c-mount, and this unit was suspended about 25 cm above the coaxial spinneret. Additionally, an external portable headlight (Fenix, model: HL23, 150 lumen) was arranged in front of the spinneret to illuminate the coaxial flow while decreasing the brightness setting in the camera software. This is why some of the backgrounds of the coaxial Taylor cone images appear dark (the experiments were all conducted in a room with normal white light). The strong scattering characteristic of an unaligned bulk nematic phase[9] makes each LC easy to distinguish from the clear, isotropic polymer solution, provided that the mixing with the sheath fluid is not too strong.

3. RESULTS

3.1. Non-Coaxial PVP−Ethanol Taylor Cone in High Humidity. While here we use ethanol as solvent for PVP, this polymer is also fully soluble in water. If the RH is high, water will condense onto the Taylor cone as it cools because of ethanol evaporation, and one might expect that the water condensation would simply make the PVP solution more fluid, without adversely affecting the Taylor cone. Indeed, between 27 and 65% RH, the spinning process is stable. A continuous single jet ejects from a steady, non-dripping Taylor cone to produce dry, well-defined, and non-meshed PVP fibers, as shown in Figure 1a−c and Movies S1, S2, and S3. The scanning electron microscopy (SEM) images of the fibers reveal no significant external morphological variations. The corresponding images of the Taylor cone reveal half-angles from the apex to the base that decrease from 41° at RH = 37% to 34° at RH = 65%, an ideal range for promoting fiber formation[22,36−38] (see the Supporting Information for details).

However, if the RH is raised to ∼72% (Figure 1d and Movie S3), the Taylor cone loses stability and deforms, with negative consequences for the fiber spinning process. In studying the dynamic behavior of the Taylor cone (Movie S3), we see signs of the polymer separating from the solution as a gel-like skin. This forming skin temporarily causes the Taylor cone to elongate into a tubular shape, followed by tip deformation, the jet pulsing in random directions, and finally, the ejection of two jets simultaneously. If not for the electrical potential being turned off in Movie S3, the fluctuating Taylor cone would have continued to eject multiple jets and intermittently pulse. We can thus conclude that a RH greater than ∼70% renders electrospinning of pure PVP fibers unreliable, not because the water keeps the jet in a fluid state, but—on the contrary—because the water condensation dries out the polymer solution in the Taylor cone before it has been spun out as a jet. We will return to discuss the origin of this phenomenon in Section 4.1;

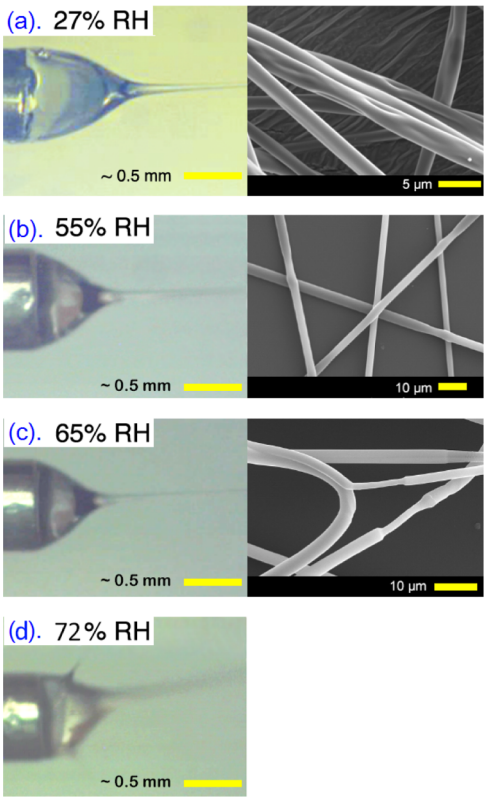

Figure 1. Video frames of the Taylor cone (left; from Movies S1, S2, and S3) together with corresponding representative SEM images (right) showing the morphology of fibers electrospun from a solution of 12.5 mass-% PVP in anhydrous ethanol in environments with low, 27% (a), and high, >50% (b−d), RH. A stable, non pulsing, and axisymmetric Taylor cone for each set of fibers produced up to RH = 65% has the following half-angles (a) 41.1, (b) 39.5, and (c) 33.9°. (The brightness and contrast of the Taylor cone images were slightly enhanced to provide better visibility of the cone profiles.)

but first, we will see how the situation can dramatically worsen in case of coaxial electrospinning, for which even lower levels of humidity can disrupt the fiber production catastrophically.

3.2. Coaxial LC-In-PVP + Ethanol Taylor Cone in High Humidity. At first glance, one might expect that a core fluid within a Taylor cone will not impact the cone's sensitivity to humid air while coaxially electrospinning or spraying because it is only the sheath solution that is in direct contact with air. The truth turns out to be quite different: depending on which core fluid is injected, the maximum acceptable RH may drastically decrease, deteriorating the Taylor cone and rendering the spinning process at even moderate RH levels impossible. An example of a core that has this effect is 5CB (probably the most commonly employed LC in research), as demonstrated in Figure 2. The figure shows the Taylor cone with 5CB injected into a standard anhydrous-ethanolic PVP sheath solution, at RH = 24 and 63%, respectively. The dynamic process is shown in Movies S4 and S5, respectively, in the Supporting Information. While the coaxial nature of the Taylor cone is easy to see at RH = 24%, with a single jet stably being ejected from the Taylor cone tip, the warped structure resulting at RH = 63% can hardly be considered a Taylor cone at all; rather than a well-defined coaxial two-phase flow, we see random texture variations and a large number of jets ejecting in all directions, even from behind the orifice because the liquids creep up along the outside of the metal capillary of the

https://dx.doi.org/10.1021/acsami.0c03338
ACS Appl. Mater. Interfaces 2020, 12, 26566−26576

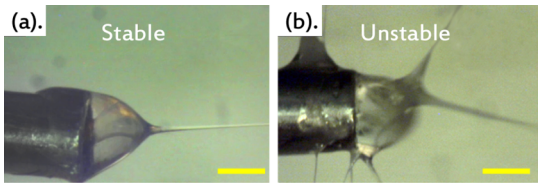

Figure 2. Screenshots of a coaxial Taylor cone with 5CB injected into a PVP−anhydrous ethanol solution, dramatically distorting from its stable, axisymmetric form with a single jet in dry air [(a) RH = 24%, supporting Movie S4] to a warped unstable shape with multiple jets and constant dripping (b) when the ambient humidity is increased to RH = 63% (supporting Movie S5). In both cases, the temperature is 23 °C. Scale bar: 0.5 mm.

spinneret. Although the PVP solution in contact with air is roughly the same as in Figure 1c, where RH is 2% higher, the result is completely different. By introducing the 5CB core, the Taylor cone becomes much more sensitive to moisture in the air, RH > ∼50% rendering coaxial electrospinning impossible.

What is going on? To test whether the liquid crystallinity of the core is the problem, we conducted a series of spinning tests at high RH, where the cores used were, respectively, 5CB, E7, and ROTN-403. The much higher clearing points of the two mixtures, compared to 5CB, means that they have *stronger* liquid crystalline character. Figure 3 shows sequential screenshots of the first 33 s of Taylor cone evolution just before commencing, and directly at the start of, the electrospinning process once the electrostatic potential is applied to the co-flowing PVP−ethanol sheath solution with 5CB, E7 and ROTN-403 core, respectively. The potential is applied by switching on the power supply, already set to 9.5 kV; thus, there is a discrete potential jump rather than a continuous ramping-up from 0 V as is otherwise often the case during electrospinning. All experiments are conducted at RH ≈ 64%. For reference, the corresponding images for the PVP−ethanol solution without any core are shown in the first row. The images shown are still frames from Movies S2 (row a), S6 (row b), and S7 (rows c, d) in the Supporting Information.

What is immediately clear is that the catastrophic spinning failure is only seen with 5CB in the core. While a few small side jets and minor distortions of the Taylor cone do occur with E7 and ROTN-403 cores, a primary jet remains stable, allowing continuous fibers with good LC core−polymer sheath geometry to be produced. With ROTN-403 as LC, the core−sheath separation also remains fully intact within the Taylor cone, as easily seen in Figure 3d from the difference in scattering between core and sheath phases. The ROTN-403 mainly occupies the center of the conical PVP−ethanol droplet, moving toward the front without spreading outward; hence, it is easily carried out into the coaxial jet, well contained by the PVP solution. With the E7 core, the separation between core and sheath is not as good, with considerable mixing apparently taking place within the droplet, as may be expected considering the large content of 5CB. Nevertheless, the greater nematic phase stability of the mixture supports the spinning process once the field is applied, indicating that it is not the liquid crystalline nature of the core that causes problems. In fact, it even appears to have a stabilizing effect.

Fibers can be collected for all three LC cores, even at high humidity, but the quality varies greatly, as shown in Figure 4. Optical microscopy reveals well-formed beaded and non-beaded coaxial PVP fibers containing E7 (b) and ROTN-403 (c) in the cores. In contrast, the fibers spun with 5CB core at this humidity level are ill-formed and partially fused, and most of the 5CB is deposited directly on the substrate, outside the fibers.

Another interesting observation in Figure 3 is that it is only with the 5CB core that the Taylor cone wets the outside of the electrified coaxial spinneret, as shown in Figure 2. The droplet creeps back some 5−6 mm along the metal capillary before it gets so large that gravitational pull detaches it. This is not seen with any of the other combinations. To further study this difference, we filmed the behavior of the protruding droplet also without applying an electric field, as shown in Figure 5. The still frames show droplet production within 10 s, taken from supporting Movies S8 (5CB), S9 (E7), and S10 (ROTN-403), respectively. In each case, the drop shown is not the first, but the second drop to emerge from the capillary. The drop containing 5CB is the only one that does not cleanly detach from the capillary orifice. While the same difference in wetting is seen also at low RH, the consequences of the wetting are much more severe if RH > ∼60% because the residues that apparently form on the sides of the metal capillary dry much

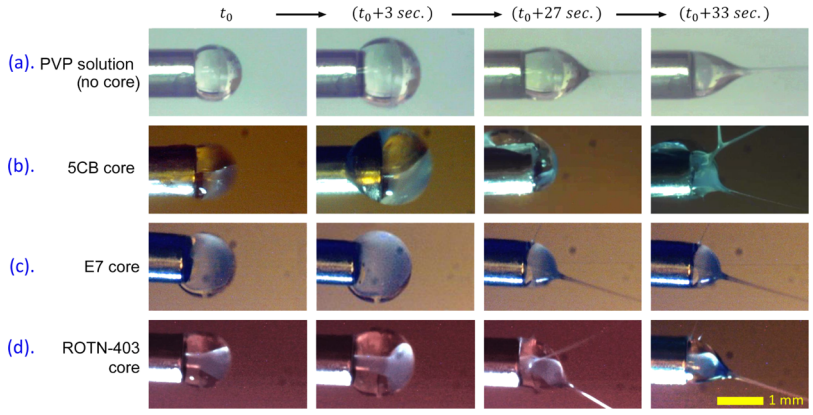

Figure 3. Evolution of the Taylor cone over the first 33 s after a fresh droplet emerges at the coaxial spinneret orifice (time t_0, first column), with the electric field turned on abruptly at $t = t_0 + 27$ s (third column). Row (a) shows the pure PVP-in-anhydrous ethanol mixture spun at 65% RH. The same PVP−ethanol solution is used as sheath in the following rows, where an LC core is injected, comprised of 5CB (b), E7 (c), and ROTN-403 (d), respectively. In rows (b−d), RH is 64%. The spinning is conducted horizontally, with the camera filming the process from the top. Gravity thus acts into the paper plane.

https://dx.doi.org/10.1021/acsami.0c03338
ACS Appl. Mater. Interfaces 2020, 12, 26566−26576

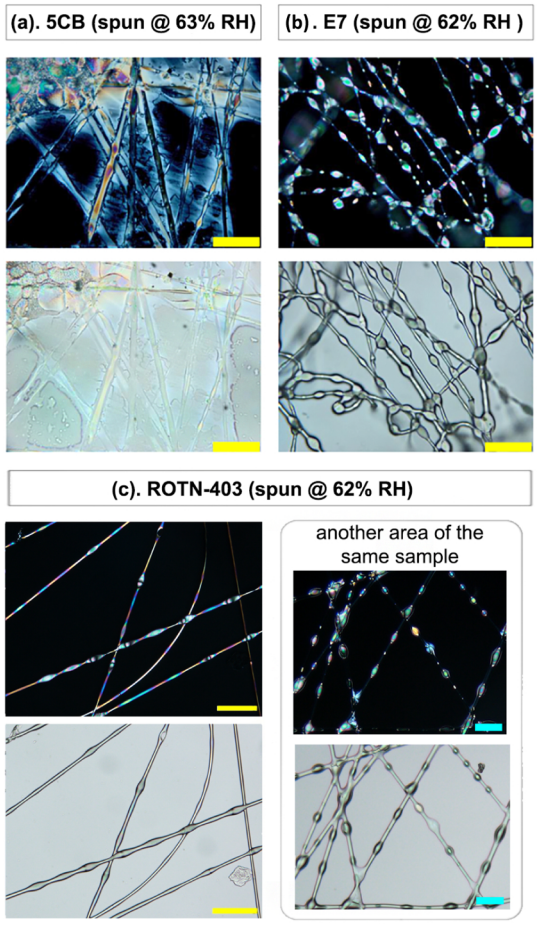

Figure 4. Polarizing optical microscopy images (top rows: crossed polarizers; bottom rows: analyzer removed) of fibers resulting from coaxial electrospinning at RH = 62−63% of the ethanolic PVP solution as sheath and LCs 5CB (a), E7 (b), and ROTN-403 (c), respectively, as the core. Scale bars: 50 μm (yellow), 100 μm (blue).

faster, leaving behind a sticky, nontransparent film of polymer mixed with 5CB.

4. DISCUSSION

4.1. Non-Coaxial Case: Water Condensation Accelerates Ethanol Evaporation and Deteriorates Solvent Quality. While a popular study by De Vrieze et al.[39] already reported that PVP−ethanol solutions cannot be reliably electrospun in humid atmospheres (RH > 60%), the behavior of the Taylor cone was not examined. The authors focused solely on the jet and the final fibers produced, reasoning that condensed water mixes into the spinning solution, dilutes it, and delays the drying of the hygroscopic PVP polymer jet. At high humidity, the still wet jet cannot solidify completely before landing on the collector, thus, creating a film of fused wet PVP fibers. If one only has access to data such as Figure 4, this conclusion is perfectly understandable, but we now know that water condensation impacts the spinning much earlier than the flight of the jet, already at the Taylor cone stage.

In our study, we use 3.6 times higher molar mass PVP than that used by De Vrieze et al., ensuring that sufficient polymer chain entanglements are achieved to sustain coaxial spinning.[28,40−42] However, it also increases the demands on the solvent quality and this is, in fact, the first critical impact of the water condensation. As demonstrated by Guettari et al.,[43] ethanol is a good solvent for PVP (chains take on an expanded coil conformation) while water is a theta solvent (ideal chain conformation) at 25 °C, but the solvent quality always *deteriorates* when the two solvents are mixed. The effect is dramatic, the polymer−polymer interaction parameter becoming negative (attractive) for molar fractions of ethanol 0.1−0.35, meaning that the polymer chains undergo a coil-to-globule transition if the water content in ethanol reaches this critical mixing regime.

The problem is further aggravated by the fact that water condensation at high RH counterintuitively *accelerates* the evaporation of ethanol. Latent heat is released when water vapor from the air condenses into the liquid of the Taylor cone, driven by the initial cooling of the latter when ethanol first evaporates. At the same time, heat is also released from the exothermic mixing reaction of water and ethanol. This surprisingly complex process was studied quantitatively by Law et al., investigating the time it took to evaporate methanol

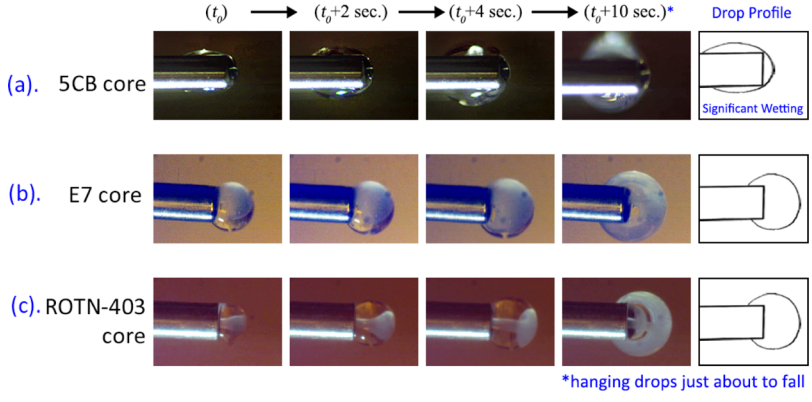

Figure 5. Droplets containing the PVP−anhydrous ethanol solution being slowly pumped out through the metal capillary to form the outer sheath, while the inner silica tube of the coaxial spinneret injects 5CB (a), E7 (b), and ROTN-403 (c), respectively, as a function of time t after the detachment of a previous drop at $t = t_0$. The coaxial spinneret is horizontal, and it is filmed from above; hence, gravity promotes the droplet hanging below the capillary, eventually detaching along a direction into the paper plane. RH = 65% in all images and no electric field is applied. With E7 and ROTN-403 cores, the droplets do not wet the edge of the capillary. They grow in size until pulled away by gravity because of their own weight. This starkly contrasts the behavior of PVP−ethanol droplets into which 5CB is injected, where the compound droplet creeps back along the capillary on both sides. Screenshots correspond to Movies S8, S9, and S10 in the Supporting Information.

https://dx.doi.org/10.1021/acsami.0c03338
ACS Appl. Mater. Interfaces 2020, 12, 26566−26576

and ethanol droplets of controlled volume in environments that were either completely dry (RH = 0%) or saturated with varying levels of moisture (RH = 65%, 73% and 100%, respectively).[44,45] In particular, the two values at 65 and 73% RH are very relevant for comparisons with our study.

Law et al. found that the temperature of a droplet of methanol formed at RH = 65% rapidly decreases from 300 to ∼277 K in about 10 s, after which the temperature gradually increases again, until reaching about 287 K after another 2 min. The reason for this variation is that, initially, the droplet, which in the study was not replenished after production, rapidly cools because it must provide latent heat for methanol evaporation. However, the decrease in temperature promotes water from the humid air to condense onto the droplet, which then *releases* latent heat. The effect is significant because of the very high specific latent heat of water, 2.26 MJ/kg at standard pressure, 2.6 times that of ethanol, 0.86 MJ/kg. This is the reason for the temperature in the droplet increasing after 10 s of initial cooling.

The temperature variation correlates very well with the evaporation rate of the droplet, which was monitored as a function of time by Law et al. for slightly higher humidity, RH = 73%. During the first 30 s, the methanol evaporated *faster* than it would in dry air at the start of the process. The overall behavior was explained by the latent heat provided by the condensing water primarily being used for evaporating the more volatile methanol and only secondarily for heating up the droplet. The evaporation rate of the droplet in high humidity eventually became slower than in dry air because the water content continuously increased through condensation, the droplet consisting of *only* water after about 2.7 min. While the experiments on ethanol droplets were not as detailed, the data show that the effects are significant also with ethanol in humid air. Law et al. found high volatility as well as miscibility with water to be critical for the effect to occur, nonpolar solvents such as hexane showing almost no influence by the ambient humidity, despite high volatility. An aspect not considered by Law et al., which should further enhance the effect is the additional heat released from the exothermic mixing of water diffused into ethanol or methanol.

The non-coaxial Taylor cone in our electrospinning experiment, initially comprising 87.5% ethanol by mass, will undoubtedly experience similar effects of water condensation and mixing at the surface, especially if exposed to humidity above ∼60%. The diameter of the hanging drop seen before electrospinning, and the widest part of the Taylor cone it transforms into, is roughly 1 mm, very similar to the droplets studied by Law et al. However, two significant differences between our study and that of Law et al. exist. First, in our study, the content of the hanging drop which converts to a Taylor cone during electrospinning is continuously replenished with fresh ethanol from the flowing PVP solution; hence, the orifice likely has a constant cold ethanol rich surface onto which water rapidly condenses as this surface flows forward to the tip of the Taylor cone. In that process, we can always expect very rapid ethanol evaporation, as in the initial stages of droplet evaporation in the studies by Law et al. Second, because we extrude a concentrated ethanol solution of high molar mass PVP that is close to its gelation point (necessary for enabling fiber formation), the PVP concentration increases as the ethanol evaporates along the Taylor cone surface. We thus have the triple critical effects of (1) the polymer concentration increasing prematurely (before jet formation), (2) water being introduced to the solution with a consequent reduction of solvent quality, and (3) this reduction being sped up by the evaporation of the ethanol. It is now easy to understand why we may quickly reach a situation where the solution no longer easily flows, essentially gelling. This is the reason why we see periodic tubular elongations of the Taylor cone in Movie S3, followed by the cone pulsing and eventually multiple jets emerging from the gelled droplet front.

These conclusions are by no means restricted to the case of PVP dissolved in ethanol. The observations of Law et al. on solvent evaporation enhanced by water condensation should apply to any volatile solvent miscible with water, such as tetrahydrofuran (THF, specific latent heat at standard pressure 0.41 MJ/kg) or acetone (0.52 MJ/kg), and as water is an extreme solvent in terms of its four hydrogen bonds per molecule, we can expect strong effects on solvent quality also in other solvent−water mixtures, similar to the case of ethanol−water.[43] We note, for instance, that Yan and Yu[46] and Yan et al.[47] reported a greatly distorted Taylor cone when spinning solutions of cellulose acetate with acetone as dominant solvent at high ambient humidity (RH > 60%). The authors overcame their problems by replenishing their actively spinning solution with excess solvent spun as a sheath around the spinning solution, but a simpler solution might have been to reduce the atmospheric humidity. We hope that our study can contribute to raising the awareness of the impact of atmospheric humidity on the stability of the Taylor cone and thus prompt follow-up studies allowing the generality of the effect for electrospinning to be assessed.

It is also interesting to compare our results with previous studies of electrospinning of water-*insoluble* polymers at high humidity nevertheless dissolved in water-miscible solvents such as THF and dimethylformamide (DMF). Based on the Law et al. studies, especially, the volatile THF should promote significant water condensation yet the water will here act as a nonsolvent for the polymer, in contrast to our case of being a theta solvent for PVP. Casper et al.[48] and Lu and Xia[49] both carried out systematic studies of polystyrene fibers electrospun from THF and/or DMF solutions as a function of ambient humidity. Regrettably, neither report gave any information about the Taylor cone; most of the experiments were carried out at humidity lower than the 72% found to be critical in our study. While the maximum humidity studied by Casper et al. was a broad RH range from 60 to 72%, Lu and Xia did not go beyond RH = 62%. Nevertheless, both studies found profound impact of humidity, in the form of a highly porous structure, increasing in prominence with rising RH, that can be traced back to phase separation induced by the presence of water as a nonsolvent.

While both studies attributed the porosity to water condensing onto the jet during flight, we believe, at least when the highly volatile THF is used, that the water condensation must have started already in the Taylor cone. The water nonsolvent would thus be present in the jet already as it leaves the Taylor cone, and the phase separation yielding the porous fiber surface morphology would result from the nonsolvent to solvent ratio rapidly increasing as THF leaves the jet. Indeed, Huang et al. used exactly this type of nonsolvent-assisted phase separation, adding the nonsolvent in a controlled fashion already to the original polymer solution, to create highly porous or surface-modulated spheres as well as fibers of polycaprolactone by electrospraying and electrospinning, respectively.[50] Their porous surface morphologies are

https://dx.doi.org/10.1021/acsami.0c03338
ACS Appl. Mater. Interfaces 2020, 12, 26566−26576

very similar to those of the fibers produced by Casper and by Lu and Xia, respectively. We may speculate that the reason that neither Casper nor Lu and Xia reported data for higher atmospheric humidities could have been that spinning failed at higher humidities, at least for the case of THF-dissolved polymer. Considering the observations of Law et al. and our own observations here, this could be expected, as strong water condensation into the Taylor cone at high humidity could lead to premature phase separation prior to jet ejection, because of the concentration of nonsolvent within the Taylor cone becoming too high.

In summary, the idea that electrospinning fails in humid environments because of water condensation onto the jet in flight, diluting a jet with the water-soluble polymer and preventing it from drying into solid fibers, or causing phase separation in the case of the water-insoluble polymer is valid but incomplete. Although water indeed condenses onto the jet, if it forms, it does so already at the stage of the Taylor cone, where the impact may be much more critical. From the studies by Law et al. we know that water condensation onto a water-miscible solvent can release so much latent heat that the rate of solvent evaporation *increases*, and even if water is a solvent for the polymer, the mixed solvent may not be so. In our case, the effect is the formation of a gel-like skin of overconcentrated PVP solution that prevents controlled electrospinning. The same argument holds for water condensation on the jet in flight, but here the impact is different, as the jet has already formed and the much greater surface-to-volume ratio also affects the process. Such differences may be worth studying in the future using computer simulations, as jet diameters exponentially reduce and are quite dynamic.

4.2. Coaxial Case: Miscibility Gaps between Co-Flowing Fluids Cause Polymer Gelation throughout the Taylor Cone. Figure 3 and the corresponding movies clearly show that the introduction of a liquid crystalline core fluid makes the Taylor cone even more sensitive to humidity, acceptably in the case of E7 or ROTN-403, catastrophically in the case of 5CB. We first analyze the former two cases. Both mixtures are partially miscible with ethanol, in particular E7, as it is comprised of roughly 50% 5CB. However, a phase boundary between the isotropic PVP solution on the outside, near the orifice, and the scattering nematic phase in the middle is always clearly visible in Movie S7. Even if the internal interface between the LC core and PVP sheath solution is somewhat blurred by their partial mixing, the Taylor cone retains a coaxial two-phase structure throughout the spinning process. This partial miscibility with ethanol, and the fact that no LC is a solvent for PVP, allows the LC in the core to act somewhat like an "internal coagulation bath", as in traditional wet spinning processes, which draws some solvent from the sheath solution into the core. Such core fluid-induced internal polymer coagulation has been reported to stabilize tubular fibers produced by coaxial electrospinning,[51,52] and Luo and Edirisinghe even reported that the effect can trigger fiber spinning, where the same polymer solution in the absence of a core only leads to electrospraying.[53] While all these studies were carried out at low to moderate humidity and no report discussed potential impact of water condensation into the Taylor cone, these reports make it perfectly understandable that coaxial electrospinning with ROTN-403 and E7 cores is successful.

But why is the situation so dramatically different with 5CB in the core? In this case, there is no visible phase boundary between the isotropic PVP solution and the nematic LC. Instead, the whole Taylor cone scatters light similar to milk. While an unaligned nematic phase shows such scattering, this should not be misunderstood as if the whole droplet were nematic. Quite on the contrary, the droplet is largely isotropic, as the clearing point of 5CB is so low that nematic order is already lost with rather little ethanol diffusing into the core. The scattering instead arises because of strong separation into multiple distinct isotropic liquid phases with different refractive indices that spread throughout the Taylor cone. Apart from the optical scattering evidence, we base this conjecture on a previous study of ours of mixtures of 5CB and ethanol.[54] It turns out that the 5CB−ethanol mixture diagram has a very large miscibility gap, which in the presence of a small amount of water (see below) spans a molar mixing ratio range of almost 50% at room temperature, as shown in Figure 6. The

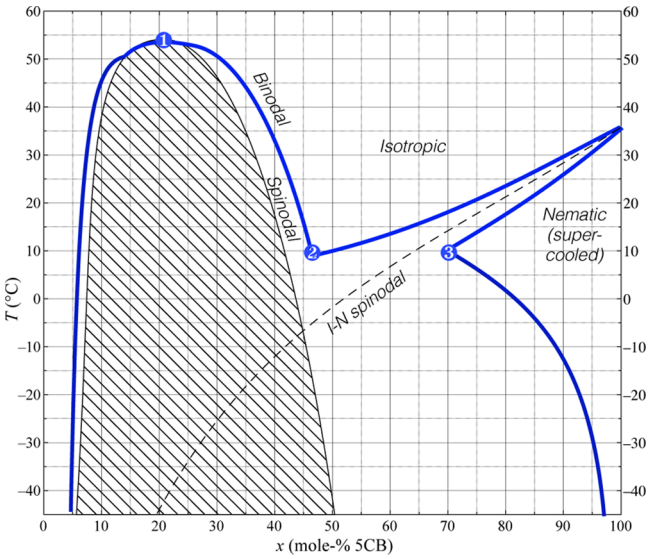

Figure 6. Phase diagram for 5CB in aqueous ethanol, that is, anhydrous ethanol with 3 vol % water added, as a function of mixing ratio and temperature. The three points of interest highlighted indicate the critical point of spinodal decomposition between the two isotropic liquid phases (1), the eutectic point of the intermediate isotropic phase, also the lowest temperature of equilibrium for the coexisting isotropic phases (2), and the lowest 5CB content possible for a 100% nematic LC phase (3). Reprinted in part with permission from ref 54. Copyright 2019 Royal Society of Chemistry.

large gap between the binodal lines in the phase diagram triggers phase separation between two different isotropic phases, one containing a lower fraction of water and ethanol and more 5CB, the other being rich in ethanol. However, while both phases are isotropic, they also contain all three liquid components, and even the "ethanol-poor" phase contains some 50 mol % ethanol. This must of course come from the original ethanol solution; hence, very strong flows are initiated by the phase separation, causing significant concentration gradients and a highly dynamic behavior.

In the electrospinning situation, also the PVP is added to the mixture. As described in much detail, in our previous work,[54] the phase separation is rapid, on a time scale much faster than the slow dynamics of a very high molar mass polymer solution. Strong concentration gradients arise throughout the Taylor cone as the phase separation produces many small droplets of new liquid phases; see the illustration in Figure 7. There will be

https://dx.doi.org/10.1021/acsami.0c03338
ACS Appl. Mater. Interfaces 2020, 12, 26566−26576

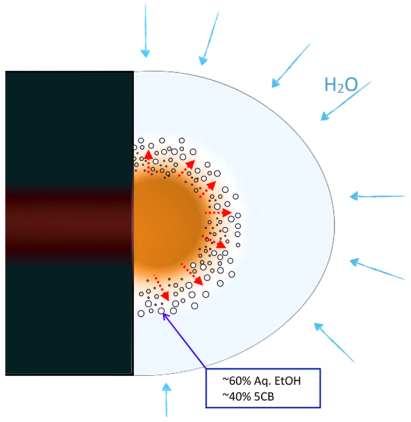

Figure 7. Diagram showing nucleating droplets of a new isotropic phase at the interface between the core 5CB fluid and the outer PVP–ethanol solution as they meet at the orifice of the coaxial needle. Water vapor from the humid atmosphere condenses onto the surface of the drop containing ethanol, diffuses through, and eventually reaches the 5CB core. This brings the composition at the interface to a region of the ternary phase diagram, where a significant miscibility gap exists, as illustrated in Figure 6, leading to many nucleating internal droplets, with varying compositions of 5CB, ethanol, and water. The PVP is localized throughout the Taylor cone except in the freshly injected LC, the polymer concentration varying strongly with location because of the strong solvent flows.

sudden jumps from about 90% ethanol in one isotropic phase to about 50% in the other one, to some 20% in regimes that maintain a composition giving nematic order. As a consequence, some regions will locally have very high PVP concentration, to the point where PVP is likely to precipitate or at least gel. Because small nucleating new phases may also prefer to form without dissolved PVP (this is suggested by complementary experiments described in the Supporting Information), the polymer may also find itself squeezed into regions between growing nuclei, effectively creating a network of the coagulated polymer. The overall result is very rapid gelation of PVP solution throughout the formation of Taylor cone, near the core as well as at the surface, yielding strong shape distortions with the applied electric field, with jets ejecting in all directions. Moreover, the strong wetting of the 5CB–ethanol mixture, most likely a result of the phase separation carrying a 5CB-rich phase with low surface energy (5CB has a weak amphiphilic character; see its molecular structure in the Supporting Information) in contact with the metal capillary, extends the surface area. This speeds up solvent evaporation, drying out the polymer even further. We no longer have a well-defined core–sheath structure in the Taylor cone, and the spinning process is out of control.

Note that this detrimental form of phase separation can only be reached at temperatures below 0 °C if no water is present.[54] This explains why the spinning is quite stable at low RH: such a low temperature is not met when spinning in dry air, allowing successful fiber production from a Taylor cone that remains coaxial. However, the effect of even a very small amount of water is dramatic: as little as 3–4 vol % of water allows the phase separation to occur at room temperature and well above, as high as up to ∼55 °C.[54] This is also why the impact of air humidity is so extreme when 5CB is in the core, as it enables the phase separation at the temperature of the experiment, while significantly lower temperatures would be required without water.

The highly dynamic phase separation process is impossible to investigate during electrospinning; so to support our conjecture, we have conducted a number of controlled reference experiments. First, without any electric field, we slowly pump an anhydrous ethanolic PVP solution (containing 12.5 mass-% PVP, the same used during electrospinning) through a vertical glass capillary until it hangs from the capillary orifice without detaching and then the flow is stopped; see Figure 8 and supporting Movie S11. The

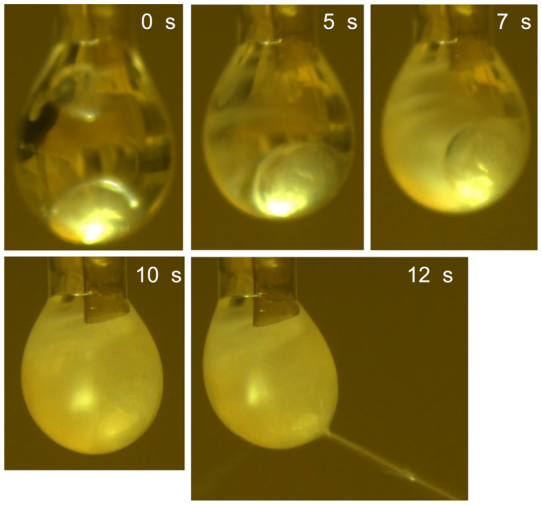

Figure 8. Phase separation seen in a hanging drop of PVP–anhydrous ethanol solution containing two small droplets of 5CB, suspended in humid air (RH = 63%). The droplets of 5CB are injected at time t = 0 s. In 10 s, the whole droplet turns into a scattering state and a sticky gel-like PVP skin forms, shown by droplet deformation and fiber formation after a needle pokes the structure and moves away in the t = 12 s frame. The whole sequence, including the needle poking the droplet, is shown in Movie S11.

surrounding air is quite humid, with RH = 63%. Through an internal piece of silica tubing, two small drops of 5CB are now injected into the PVP solution droplet and we then study the development.

Initially, the heavier nematic 5CB droplets sink to the bottom, but over the course of a few seconds, mixing with ethanol as well as water condensing from the air triggers the phase separation. This is seen as a hazy white fog spreading from one corner of the compound droplet to the other, which soon becomes entirely milky. Touching the droplet with a needle at this point, only some 10 s after injecting the 5CB, shows that the PVP has indeed gelled, becoming sticky and rubber-like. The droplet does not break or detach but simply deforms and rebounds in response to the mechanical disruption, eventually even making threads as the needle moves away. Additional support of our interpretation is provided by optical microscopic investigations of 5CB carefully brought into contact with an aqueous PVP-in-ethanol solution, as well as a long-term experiment (2 months) of the phase separation with PVP present taking place in a separatory funnel. Both experiments are described in the Supporting Information.

5. CONCLUSIONS

From our systematic study examining how ethanolic polymer solutions are electrospun in high humidity, with and without

https://dx.doi.org/10.1021/acsami.0c03338
ACS Appl. Mater. Interfaces 2020, 12, 26566–26576

LC core liquids, and the corresponding Taylor cone behavior, we conclude that the impact of ambient humidity goes far beyond influencing the ejected jet. High humidity has the potential to distort or even completely disrupt the Taylor cone, making the electrospinning process unsustainable and uncontrollable. Without a stable cone, the uniformity of the jet, and thus, fiber formation, cannot be ensured. The reason for the instability is the condensation of liquid water onto the ethanol-dissolved polymer because of the cooling down of the Taylor cone as volatile ethanol evaporates. The water condensation releases significant latent heat which accelerates ethanol evaporation, and it strongly deteriorates the quality of the solvent, to the extent that polymer precipitates as a gel-like skin around the Taylor cone. This polymer skin ultimately interferes with the replenishment of liquid needed to sustain the Taylor cone and jet ejected from it.

When a core liquid that forms a complex phase diagram with ethanol and water is co-flowed into the Taylor cone, the effect can render coaxial electrospinning impossible at humidity levels, where the polymer solution on its own can safely be spun. We find that if a miscibility gap exists in the phase diagram of the components mixing at the core−sheath interface, many strong gradients in ethanol concentration may arise between adjacent nucleating phases when the original phase breaks down. The polymer concentration will locally increase drastically, causing coagulation and gelation internally that clogs the electrospinning process. Although this was demonstrated using a liquid crystalline substance as the core, its liquid crystalline nature was not the culprit. In fact, this aspect had a stabilizing effect, as demonstrated with LC mixtures with higher clearing points causing no significant problems. Ultimately, the critical issue is if a miscibility gap arises or not between the components combined, hence similar phenomena while electrospinning may be expected to also occur with non-liquid crystalline core liquids.

■ ASSOCIATED CONTENT

Supporting Information

The Supporting Information is available free of charge at https://pubs.acs.org/doi/10.1021/acsami.0c03338.

Miscibility of the three LCs (5CB, E7, and ROTN-403) in six common laboratory grade solvents, reference experiments on phase separation when 5CB is mixed with aqueous ethanolic PVP solutions, in the polarizing microscope and at macroscopic scale over long time, discussion of the effects of water condensation on surface tension, dielectric permittivity and conductivity, and descriptions of the experimental setup including schematics/photos (PDF)

Video of a continuous single jet ejecting from a steady, nondripping Taylor cone at 55% RH (MOV)

Video of a continuous single jet ejecting from a steady, nondripping Taylor cone at 65% RH (MOV)

Video of single-fluid electrospinning breaking down at the Taylor cone at 72% RH (MOV)

Video of stable 5CB core-PVP-in-ethanol sheath spinning at 24% RH (MOV)

Video of 5CB core-PVP-in-ethanol sheath spinning breaking down at 63% RH (MOV)

Video of 5CB core-PVP-in-ethanol sheath spinning at 64% RH (MOV)

Video of E7 and ROTN-403 core, respectively, and PVP-in-ethanol sheath spinning at 64% RH (MOV)

Video of 5CB core-PVP-in-ethanol sheath pumped without electric field, wetting the spinneret outside (MOV)

Video of E7 core-PVP-in-ethanol sheath pumped without electric field, with no significant spinneret wetting (MOV)

Video of ROTN-403 core-PVP-in-ethanol sheath pumped without electric field, with no significant spinneret wetting (MOV)

Video of 5CB injected into a PVP-in-ethanol solution at 63% RH inducing phase separation, rapidly yielding strong scattering and the formation of sticky gel-like PVP skin (MOV)

■ AUTHOR INFORMATION

Corresponding Author

Jan P. F. Lagerwall − *Department of Physics and Materials Science, University of Luxembourg, Luxembourg L-1511 Luxembourg;* orcid.org/0000-0001-9753-1147; Phone: (+352) 46 66 44 6219; Email: jan.lagerwall@lcsoftmatter.com; Fax: (+352) 46 66 44 36219

Author

Catherine G. Reyes − *Department of Physics and Materials Science, University of Luxembourg, Luxembourg L-1511 Luxembourg;* orcid.org/0000-0002-1289-9717

Complete contact information is available at: https://pubs.acs.org/10.1021/acsami.0c03338

Notes

The authors declare no competing financial interest.

■ ACKNOWLEDGMENTS

The authors thank Dr. Manos Anyfantakis and Shameek Vats for pointing us to valuable literature regarding properties of water−ethanol mixtures previously unknown to us. Financial support from the European Research Council under the European Unions Seventh Framework Programme (FP/2007−2013)/ERC grant agreement no. 648763 (consolidator project INTERACT) is gratefully acknowledged.

■ ADDITIONAL NOTES

[a]The value in the paper was written 11.86 ms/cm, but we assume that there is a typo in the unit.

[b]We are uncertain about the reliability of this value, as it not only is 1−2 orders of magnitude lower than the values in the other papers but the same paper also, in fact, reports a conductivity of 7.6 μS/cm for a 10% solution of PVP with M_w = 0.55 × 10^6 g/mol.

■ REFERENCES

(1) Xue, J.; Wu, T.; Dai, Y.; Xia, Y. Electrospinning and Electrospun Nanofibers: Methods, Materials, and Applications. *Chem. Rev.* **2019**, *119*, 5298−5415.

(2) Zhang, S.; Campagne, C.; Salaün, F. Influence of Solvent Selection in the Electrospraying Process of Polycaprolactone. *Appl. Sci.* **2019**, *9*, 402.

(3) Reneker, D. H.; Yarin, A. L. Electrospinning Jets and Polymer Nanofibers. *Polymer* **2008**, *49*, 2387−2425.

(4) Wang, C.; Wang, M. Electrospun Multicomponent and Multifunctional Nanofibrous Bone Tissue Engineering Scaffolds. *J. Mater. Chem. B* **2017**, *5*, 1388−1399.
(5) Zhang, C.; Li, Y.; Hu, Y.; Peng, Y.; Ahmad, Z.; Li, J.-S.; Chang, M.-W. Porous Yolk−Shell Particle Engineering via Nonsolvent-Assisted Trineedle Coaxial Electrospraying for Burn-Related Wound Healing. *ACS Appl. Mater. Interfaces* **2019**, *11*, 7823−7835.
(6) Zhou, F.-L.; Wu, H.; McHugh, D. J.; Wimpenny, I.; Zhang, X.; Gough, J. E.; Hubbard Cristinacce, P. L.; Parker, G. J. M. Co-Electrospraying of Tumour Cell Mimicking Hollow Polymeric Microspheres for Diffusion Magnetic Resonance Imaging. *Mater. Sci. Eng., C* **2019**, *101*, 217−227.
(7) Khalf, A.; Madihally, S. V. Recent Advances in Multiaxial Electrospinning for Drug Delivery. *Eur. J. Pharm. Biopharm.* **2017**, *112*, 1−17.
(8) Yang, Y.; Li, W.; Yu, D.-G.; Wang, G.; Williams, G. R.; Zhang, Z. Tunable Drug Release from Nanofibers Coated with Blank Cellulose Acetate Layers Fabricated using Tri-Axial Electrospinning. *Carbohydr. Polym.Carbohydrate Polymers* **2019**, *203*, 228−237.
(9) Urbanski, M.; Reyes, C. G.; Noh, J.; Sharma, A.; Geng, Y.; Subba Rao Jampani, V.; Lagerwall, J. P. F. Liquid Crystals in Micron-Scale Droplets, Shells and Fibers. *J. Phys.: Condens. Matter* **2017**, *29*, 133003.
(10) McCann, J. T.; Marquez, M.; Xia, Y. Melt Coaxial Electrospinning: A Versatile Method for the Encapsulation of Solid Materials and Fabrication of Phase Change Nanofibers. *Nano Lett.* **2006**, *6*, 2868−2872.
(11) Wang, N.; Chen, H.; Lin, L.; Zhao, Y.; Cao, X.; Song, Y.; Jiang, L. Multicomponent Phase Change Microfibers Prepared by Temperature Control Multifluidic Electrospinning. *Macromol. Rapid Commun.* **2010**, *31*, 1622−1627.
(12) Sharma, A.; Lagerwall, J. Electrospun Composite Liquid Crystal Elastomer Fibers. *Materials* **2018**, *11*, 393.
(13) Enz, E.; Lagerwall, J. Electrospun Microfibres With Temperature Sensitive Iridescence From Encapsulated Cholesteric Liquid Crystal. *J. Mater. Chem.* **2010**, *20*, 6866−6872.
(14) Lin, J.-D.; Chen, C.-P.; Chen, L.-J.; Chuang, Y.-C.; Huang, S.-Y.; Lee, C.-R. Morphological Appearances and Photo-controllable Coloration of Dye-Doped Cholesteric Liquid Crystal/Polymer Coaxial Microfibers Fabricated by Coaxial Electrospinning Technique. *Opt. Express* **2016**, *24*, 3112−3126.
(15) Enz, E.; La Ferrara, V.; Scalia, G. Confinement-Sensitive Optical Response of Cholesteric Liquid Crystals in Electrospun Fibers. *ACS Nano* **2013**, *7*, 6627−6635.
(16) Reyes, C. G.; Lagerwall, J. P. F. Advancing Flexible Volatile Compound Sensors using Liquid Crystals Encapsulated in Polymer Fibers. *Proc. SPIE* **2018**, *10555*, 105550O.
(17) Reyes, C. G.; Sharma, A.; Lagerwall, J. P. F. Non-Electronic Gas Sensors from Electrospun Mats of Liquid Crystal Core Fibers for Detecting Volatile Organic Compounds at Room Temperature. *Liq. Cryst.* **2016**, *43*, 1986−2001.
(18) Kim, D. K.; Hwang, M.; Lagerwall, J. P. F. Liquid Crystal-Functionalization of Electrospun Polymer Fibers. *J. Polym. Sci. Part B: Polym. Phys.* **2013**, *51*, 855−867.
(19) Wang, J.; Jákli, A.; West, J. L. Liquid Crystal/Polymer Fiber Mats as Sensitive Chemical Sensors. *J. Mol. Liq.* **2018**, *267*, 490−495.
(20) Bertocchi, M. J.; Vang, P.; Balow, R. B.; Wynne, J. H.; Lundin, J. G. Enhanced Mechanical Damping in Electrospun Polymer Fibers with Liquid Cores: Applications to Sound Damping. *ACS Appl. Polym. Mater.* **2019**, *1*, 2068−2076.
(21) Taylor, G. I. Disintegration of Water Drops in an Electric Field. *Proc. R. Soc. A* **1964**, *280*, 383−397.
(22) Taylor, G. I. Electrically Driven Jets. *Proc. R. Soc. A* **1969**, *313*, 453−475.
(23) Bellan, L. M.; Craighead, H. G.; Hinestroza, J. P. Direct Measurement of Fluid Velocity in an Electrospinning Jet using Particle Image Velocimetry. *J. Appl. Phys.* **2007**, *102*, 094308.
(24) Wang, J.; Jákli, A.; West, J. L. Morphology Tuning of Electrospun Liquid Crystal/Polymer Fibers. *ChemPhysChem* **2016**, *17*, 3080−3085.
(25) Kye, Y.; Kim, C.; Lagerwall, J. Multifunctional responsive fibers produced by dual liquid crystal core electrospinning. *J. Mater. Chem. C* **2015**, *3*, 8979−8985.
(26) Buyuktanir, E. A.; Frey, M. W.; West, J. L. Self-Assembled, Optically Responsive Nematic Liquid Crystal/Polymer Core-shell Fibers: Formation and Characterization. *Polymer* **2010**, *51*, 4823−4830.
(27) Loscertales, I. G.; Barrero, A.; Guerrero, I.; Cortijo, R.; Marquez, M.; Ganan-Calvo, A. Micro/Nano Encapsulation via Electrified Coaxial Liquid Jets. *Science* **2002**, *295*, 1695−1698.
(28) López-Herrera, J. M.; Barrero, A.; López, A.; Loscertales, I. G.; Márquez, M. Coaxial Jets Generated from Electrified Taylor Cones. Scaling Laws. *J. Aerosol Sci.* **2003**, *34*, 535−552.
(29) Díaz, J. E.; Barrero, A.; Márquez, M.; Loscertales, I. G. Controlled Encapsulation of Hydrophobic Liquids in Hydrophilic Polymer Nanofibers by Co-Electrospinning. *Adv. Funct. Mater.* **2006**, *16*, 2110−2116.
(30) Teodorescu, M.; Bercea, M. Poly(vinylpyrrolidone) − A Versatile Polymer for Biomedical and Beyond Medical Applications. *Polym.-Plast. Technol. Eng.* **2015**, *54*, 923−943.
(31) Asawahame, C.; Sutjarittangtham, K.; Eitssayeam, S.; Tragoolpua, Y.; Sirithunyalug, B.; Sirithunyalug, J. Formation of Orally Fast Dissolving Fibers Containing Propolis by Electrospinning Technique. *Chiang Mai J. Sci.* **2015**, *42*, 469−480.
(32) Cengiz Çallioğlu, F.; Kesici Güler, H. Fabrication of Polyvinylpyrrolidone Nanofibers with Green Solvents. *Süleyman Demirel University Faculty of Arts and Sciences Journal of Science* **2019**, *14*, 352−366.
(33) Forward, K. M.; Rutledge, G. C. Free Surface Electrospinning from a Wire Electrode. *Chem. Eng. J.* **2012**, *183*, 492−503.
(34) Gerber, P. R. Measurement of the Rotational Viscosity of Nematic Liquid-Crystals. *Appl. Phys. A* **1981**, *26*, 139−142.
(35) Schymura, S.; Kühnast, M.; Lutz, V.; Jagiella, S.; Dettlaff-Weglikowska, U.; Roth, S.; Giesselmann, F.; Tschierske, C.; Scalia, G.; Lagerwall, J. Towards Efficient Dispersion of Carbon Nanotubes in Thermotropic Liquid Crystals. *Adv. Funct. Mater.* **2010**, *20*, 3350−3357.
(36) Yarin, A. L.; Koombhongse, S.; Reneker, D. H. Taylor Cone and Jetting from Liquid Droplets in Electrospinning of Nanofibers. *J. Appl. Phys.* **2001**, *90*, 4836−4846.
(37) Kalayci, V. E.; Patra, P. K.; Kim, Y. K.; Ugbolue, S. C.; Warner, S. B. Charge Consequences in Electrospun Polyacrylonitrile (PAN) Nanofibers. *Polymer* **2005**, *46*, 7191−7200.
(38) Barua, B.; Saha, M. C. Investigation on Jet Stability, Fiber Diameter, and Tensile Properties of Electrospun Polyacrylonitrile Nanofibrous Yarns. *J. Appl. Polym. Sci.* **2015**, *132*, 41918−41928.
(39) De Vrieze, S.; Van Camp, T.; Nelvig, A.; Hagström, B.; Westbroek, P.; De Clerck, K.; De, K. Clerck The Effect of Temperature and Humidity on Electrospinning. *J. Mater. Sci.* **2009**, *44*, 1357−1362.
(40) Shenoy, S. L.; Bates, W. D.; Frisch, H. L.; Wnek, G. E. Role of Chain Entanglements on Fiber Formation During Electrospinning of Polymer Solutions: Good Solvent, Non-Specific Polymer−Polymer Interaction Limit. *Polymer* **2005**, *46*, 3372.
(41) Hu, H.; Zhao, K.; Fernandes, N.; Boufflet, P.; Bannock, J. H.; Yu, L.; de Mello, J. C.; Heeney, M.; Giannelis, E. P.; Amassian, A.; Amassian, A. Entanglements in Marginal Solutions: A Means of Tuning Pre-Aggregation of Conjugated Polymers with Positive Implications for Charge Transport. *J. Mater. Chem. C* **2015**, *3*, 7394−7404.
(42) Aharoni, S. M. On Entanglements of Flexible and Rodlike Polymers. *Macromolecules* **1983**, *16*, 1722−1728.
(43) Guettari, M.; Belaidi, A.; Abel, S.; Tajouri, T. Polyvinylpyrrolidone Behavior in Water/Ethanol Mixed Solvents: Comparison of Modeling Predictions with Experimental Results. *J. Solution Chem.* **2017**, *46*, 1404−1417.

https://dx.doi.org/10.1021/acsami.0c03338
ACS Appl. Mater. Interfaces 2020, 12, 26566−26576

(44) Law, C. K.; Xiong, T. Y.; Wang, C. Alcohol Droplet Vaporization in Humid Air. *Int. J. Heat Mass Transfer* **1987**, *30*, 1435−1443.
(45) Lee, A.; Law, C. K. An Experimental Investigation on the Vaporization and Combustion of Methanol and Ethanol Droplets. *Combust. Sci. Technol.* **1992**, *86*, 253−265.
(46) Yan, J.; Yu, D.-G. Smoothening electrospinning and obtaining high-quality cellulose acetate nanofibers using a modified coaxial process. *J. Mater. Sci.* **2012**, *47*, 7138−7147.
(47) Yan, J.; White, K.; Yu, D.-G.; Zhao, X.-Y. Sustained-release multiple-component cellulose acetate nanofibers fabricated using a modified coaxial electrospinning process. *J. Mater. Sci.* **2014**, *49*, 538−547.
(48) Casper, C. L.; Stephens, J. S.; Tassi, N. G.; Chase, D. B.; Rabolt, J. F. Controlling surface morphology of electrospun polystyrene fibers: Effect of humidity and molecular weight in the electrospinning process. *Macromolecules* **2004**, *37*, 573−578.
(49) Lu, P.; Xia, Y. Maneuvering the Internal Porosity and Surface Morphology of Electrospun Polystyrene Yarns by Controlling the Solvent and Relative Humidity. *Langmuir* **2013**, *29*, 7070−7078.
(50) Huang, X.; Gao, J.; Li, W.; Xue, H.; Li, R. K. Y.; Mai, Y.-W. Preparation of Poly(ϵ-Caprolactone) Microspheres and Fibers with Controllable Surface Morphology. *Mater. Des.* **2017**, *117*, 298−304.
(51) Dror, Y.; Salalha, W.; Avrahami, R.; Zussman, E.; Yarin, A. L.; Dersch, R.; Greiner, A.; Wendorff, J. H. One-Step Production of Polymeric Microtubes by Co-Electrospinning. *Small* **2007**, *3*, 1064−1073.
(52) Zussman, E.; Yarin, A. L.; Bazilevsky, A. V.; Avrahami, R.; Feldman, M. Electrospun Polyaniline/Poly(Methyl Methacrylate)-Derived Turbostratic Carbon Micro-/Nanotubes. *Adv. Mater.* **2006**, *18*, 348−353.
(53) Luo, C. J.; Edirisinghe, M. Core-Liquid-Induced Transition from Coaxial Electrospray to Electrospinning of Low-Viscosity Poly(Lactide−Glycolide) Sheath Solution. *Macromolecules* **2014**, *47*, 7930−7938.
(54) Reyes, C. G.; Baller, J.; Araki, T.; Lagerwall, J. P. F. Isotropic-Isotropic Phase Separation and Spinodal Decomposition in Liquid Crystal-Solvent Mixtures. *Soft Matter* **2019**, *15*, 6044−6054.

https://dx.doi.org/10.1021/acsami.0c03338
ACS Appl. Mater. Interfaces 2020, 12, 26566−26576